Fractional quantum Hall effect at $\nu=\frac{2}{3}$ and $\frac{3}{5}$ in tilted magnetic fields

L. W. Engel, S. W. Hwang, T. Sajoto, D. C. Tsui, and M. Shayegan
Department of Electrical Engineering, Princeton University, Princeton, New Jersey 08544
(Received 26 July 1991)

We report on measurements of electron transport for the fractional quantum Hall effect (FQHE) at filling factors $\nu=\frac{2}{3}$ and $\frac{3}{5}$, in magnetic fields $\mathbf{B}_t$ tilted by angles θ with respect to the normal to the sample plane. Our device was prepared at an electron density of only 2.4×10^{10} cm^{-2}, but still exhibited a well-developed FQHE at $\nu=\frac{2}{3}$ and $\frac{3}{5}$. This exceptionally low density allowed us to access very low total fields, where the spin is less likely to be completely polarized. For many tilt angles, we obtained gap energies Δ from the temperature dependence of the diagonal conductivity on the FQHE minima. For both $\frac{2}{3}$ and $\frac{3}{5}$, plots of Δ versus B_t exhibit minima that are accompanied in transport by splitting of the FQHE. For $\frac{2}{3}$ the minimum in $\Delta(B_t)$ is sharp and deep, with Δ reduced by 70%. With B_t well above its value at the minimum, $\Delta(B_t)$ for $\nu=\frac{2}{3}$ is linear, with slope $\approx g\mu_B$ for GaAs, indicating an increase in the two-dimensional electron-system Zeeman energy on excitation. We present a detailed survey of the evolution of the splitting of the FQHE with angle, and find that local ρ_{xx} minima that are shifted up to 6% upfield of $\nu=\frac{2}{3}$ at $\theta\approx23°$ evolve continuously into an unsplit FQHE at $\nu=\frac{2}{3}$ at $\theta\approx0°$. The split and shifted FQHE's that we observe are interpreted as effects of phase separation associated with ground-state spin transitions.

I. INTRODUCTION

The fractional quantum Hall effect[1] (FQHE) is the result of a many-body interacting ground state that corresponds to an incompressible liquid. The first proposed trial wave function[2] for this ground state assumed a completely polarized system, but was shortly followed by descriptions[3–5] of spin-unpolarized ground states with the requisite properties. Most of the attention has until recently been focused on fully polarized FQHE ground states, which were assumed to be favored by the high magnetic fields required for the observation of the FQHE. Experiments have by now indicated that the ground state and excitations in the FQHE are not in general completely polarized.[6–12] Tilting the magnetic field B with respect to the sample has been a valuable method for studying the role of the spin degree of freedom in the FQHE. In principle, tilting the magnetic field allows separation of the effects of spin and of electron-electron interaction. The Zeeman energy E_Z, associated with the spin degree of freedom, depends on the total field B_t, while the Coulomb energy E_C associated with the electron-electron interaction depends only on the perpendicular field $B_\perp$, at least in the approximation[13,14] where the finite thickness of the two-dimensional electron system (2DES) is neglected. The dependence of the FQHE ground- or excited-state energies on the tilt angle at some particular filling factor ν (hence a particular $B_\perp\propto\nu^{-1}$) can then be attributed to the Zeeman term. For example, a tilted-field experiment[7] on the even-denominator FQHE at $\nu=\frac{5}{2}$ showed the energy gap to decrease with increasing B_t, in agreement with the FQHE ground state at that filling being unpolarized.

The parallel field $B_\parallel$ that is varied in a tilted-field experiment on the FQHE at some particular filling factor can also cause a transition in the ground state or in its preferred excitations. The energy gap Δ as a function of B_t for the $\frac{8}{5}$ FQHE has been observed[10] to decrease linearly when B_t is less than a critical field B_{tc}, and to increase linearly when B_t is greater than B_{tc}. The slopes, $\mp g\mu_B$, with g about 0.4 for GaAs and μ_B the Bohr magneton, are explained by Zeeman contributions to the energy gap, and the minimum in Δ vs B_t is then interpreted as resulting from a phase transition at B_{tc}, from an unpolarized, low-B_t ground state favored by E_c to a polarized, high-B_t ground state favored by E_z.

For the $\frac{2}{3}$ FQHE the interpretation of Δ vs B_t plots obtained from tilted-field experiments is more complicated. Low electron densities, which allow access to smaller B_t and smaller Zeeman energies, are important for observing spin effects. Tilted-field experiments[6,8] were first performed on samples whose densities allowed minimum B_t of ~9.0 T or more at $\nu\sim\frac{2}{3}$. As B_t was increased by tilting, the resulting Δ for $\nu=\frac{2}{3}$ increased markedly, while Δ for $\nu=\frac{1}{3}$ decreased only slightly. This is an apparent violation of electron-hole symmetry for fully polarized ground states and excitations, but a recent theoretical paper[14] shows that the different B_t dependence observed for the $\nu=\frac{1}{3}$ and $\frac{2}{3}$ gap energies can be largely explained by subband-Landau-level coupling, an effect of the finite thickness of the 2DES. Eisenstein *et al.*[11] performed an experiment on a lower-density sample, which allowed a minimum B_t of 2.5 T at $\nu=\frac{2}{3}$, and observed a well-defined minimum in Δ vs B_t at that filling. There was good reason to believe that this minimum was a spin effect, since it could be observed both by tilting the sample and by increasing the density of a sample perpendicular to the field. Clark *et al.*[12] performed a tilted-field experiment on a sample of only slightly higher density, and

observed that at fixed temperature T the depth of the $\nu\sim\frac{2}{3}$ minimum in diagonal resistivity, ρ_{xx}, was reduced over a certain range of angle, likely corresponding to a minimum in $\Delta(B_t)$. They also observed a resolved splitting of the $\nu\sim\frac{2}{3}$ ρ_{xx} minimum at the angles where that minimum was the weakest, though Eisenstein *et al.*[11] observed no such splitting. When the spin degree of freedom is included the electron-hole conjugate state of $\nu=\frac{2}{3}$ is $\nu=\frac{4}{3}$. A tilted-field experiment[9] showed the $\frac{4}{3}$ FQHE minimum in ρ_{xx} to vanish with $7<B_t<9$ T, while being observable with B_t outside of this range.

The FQHE at $\nu=\frac{3}{5}$ is weaker than the $\nu=\frac{2}{3}$ effect, and has been less extensively studied in tilted-field experiments. Working at $B_t\gtrsim 10$ T at $\nu=\frac{3}{5}$, Haug *et al.*[6] observed only a slight tilt dependence in the $\nu=\frac{3}{5}$ diagonal conductivity minima. Clark *et al.*[12] found that in a much lower density sample, the ρ_{xx} minimum at $\nu\sim\frac{3}{5}$ (at fixed T) weakened in the same range of angles as the $\nu\sim\frac{2}{3}$ minimum did. The FQHE at $\nu=\frac{7}{5}$, which is electron-hole conjugate to $\nu=\frac{3}{5}$, was found to disappear for $B_t\gtrsim 10$ T.[9]

Theoretical consideration of FQHE ground states that are not completely polarized began with the proposal[3] of an incompressible trial wave function for $\nu=\frac{2}{5}$ that has zero spin. E_C for this wave function was evaluated numerically,[4] and was shown to be lower than that for the alternative, fully polarized wave function. Exact numerical diagonalization[5] of the Hamiltonian of a small model system likewise gave a lower E_C for an unpolarized $\nu=\frac{2}{5}$ state, and indicated that at $\nu=\frac{2}{7}$, $\frac{4}{9}$, $\frac{4}{11}$, and $\frac{4}{13}$ the incompressible states with the lowest E_C would not be fully polarized. Subsequent theoretical work[15] considered the energies of spin-reversed excitations of FQHE ground states. Calculations have only recently focused on the spin degree of freedom in the ground state and excitations of the FQHE at $\nu=\frac{2}{3}$ and $\frac{3}{5}$. These calculations,[16–19] all based on exact diagonalization of small-system Hamiltonians, are in agreement that for $\nu=\frac{2}{3}$, a completely unpolarized state has the lowest E_C, so that such a ground state is in principle possible at low enough B_t. For $\nu=\frac{3}{5}$, on the other hand, the calculations[18,19] predict a partially polarized ground state.

In this paper we describe tilted-field experiments on the $\frac{2}{3}$ and $\frac{3}{5}$ FQHE in a sample whose density is much lower than in any previous tilted-field study of the FQHE. The minimum B_t at $\nu=\frac{2}{3}$ was only 1.52 T, corresponding to a per electron Zeeman energy of about 400 mK in a fully polarized state. At $\theta\sim 33°$, both the $\frac{2}{3}$ and $\frac{3}{5}$ FQHE exhibit a splitting, which is accompanied by a minimum in the corresponding energy gap Δ. We present a careful study of the evolution of this splitting with tilt angle, and find that a ρ_{xx} minimum and associated ρ_{xy} inflection, that are shifted far from $\nu=\frac{2}{3}$ at intermediate θ, can evolve into an unsplit $\nu=\frac{2}{3}$ FQHE at large and small θ. We interpret the FQHE splitting, associated with minima in Δ vs B_t, as an effect of the coexistence of two phases in a ground-state spin transition. Some features of the Δ vs B_t curves we measured are also of interest. For the $\frac{2}{3}$ FQHE, Δ vs B_t exhibits a sharp, deep minimum, at which the gap energy is only about 30% of its value at the shoulder. For B_t well above that where the minimum occurs, Δ vs (B_t) for $\nu=\frac{2}{3}$ increases linearly with slope $\approx g\mu_B$ for GaAs, implying that the Zeeman energy increases on excitation. Our Δ vs B_t plot for $\nu=\frac{3}{5}$ is the first to demonstrate a $\Delta(B_t)$ minimum.

II. DEVICE AND EXPERIMENTAL METHODS

The experiments described here were all performed on a sample of $GaAs/Al_xGa_{1-x}As$ heterojunction from wafer M73, which has been characterized elsewhere.[20] The sample was prepared by brief illumination with red light at low T. The sample states we studied had density $n\approx 2.4\times 10^{10}$ cm^{-2} and mobility $\mu\approx 7.1\times 10^5$ cm^2/V sec. We used a measuring current of 10 nA rms, and checked that any local heating at this current was negligible by comparing ρ_{xx} values measured with different currents. The sample was rotated on a spring-loaded stage in the mixing chamber of an Oxford 200 TLM dilution refrigerator. Our convention defines the angle θ as that between the normal to the sample and the field $\mathbf{B}_{\rm tot}$, so that $B_t=B_\perp/\cos\theta$. B_t was estimated from the current in a superconducting magnet, and great care was taken in cycling the magnet, so that hysteresis effects caused only a ± 0.01 T unrepeatability in our stated B_t's.

III. SPLITTING OF THE ρ_{xx} MINIMA

Figure 1 shows the diagonal resistivity ρ_{xx} vs B_t, for $\theta\approx 2.6°$ and 34°. The ρ_{xx} minima at $\nu=\frac{2}{3}$ and $\frac{3}{5}$ at 2.6° are well developed in spite of the very low fields at which we observe them. At 34° these minima appear to be weaker, and develop a pronounced splitting. The $\frac{2}{5}$ and $\frac{1}{3}$ minima remain unique and unsplit, similar to their appearance in Fig. 1, at all angles surveyed. We observed the splitting of ρ_{xx} minima only in the $\nu\sim\frac{2}{3}$ to $\frac{4}{7}$ region, and only over a narrow range of θ, so that this splitting is evidently not an effect of frozen-in macroscopic inhomogeneity of the sample density.

Figure 2 shows the evolution of the FQHE ρ_{xx} minima for ν in the $\frac{2}{3}$ to $\frac{4}{7}$ region, as θ is increased. The horizontal axis is the perpendicular field, so the traces do not shift upfield with increasing angle. Vertical lines mark $\nu=\frac{2}{3}$ and $\frac{3}{5}$. Throughout this paper, the fields that correspond to filling factors are calibrated over angle from $\rho_{xy}(B_t)$ at high T, which approximates the classical line $B_t/ne\cos\theta$. A B_t corresponding to a particular ν is therefore accurate to within our field repeatability of ± 0.01 T. At the highest and lowest angles, $\rho_{xx}(B_\perp)$ shows single, well-defined minima for $\nu\sim\frac{2}{3}$ and $\frac{3}{5}$, but in a region of intermediate angles these minima appear to be split, each into two distinct subminima. For $\nu\sim\frac{2}{3}$, the two subminima have equal ρ_{xx} at $\theta\approx 33°$. As θ is decreased from 33°, the low-$B_\perp$ subminimum evolves into the main $\nu=\frac{2}{3}$ minimum and strengthens, while the high-$B_\perp$ subminimum shifts further upfield from $\nu=\frac{2}{3}$, weakens, and eventually disappears. As θ is increased

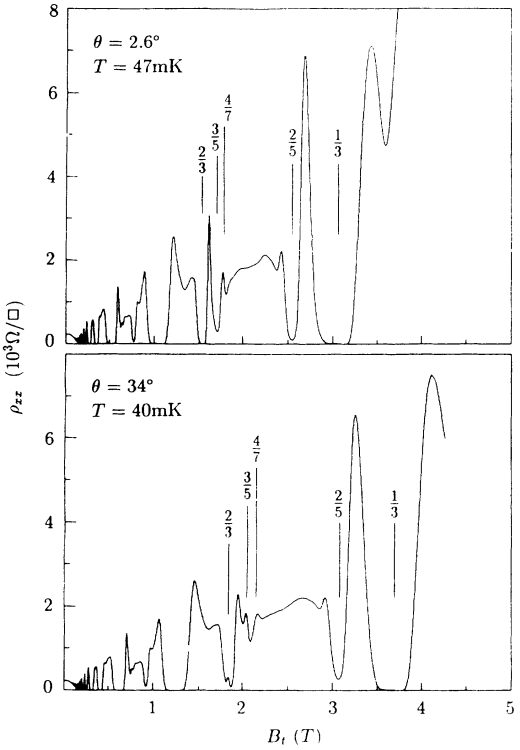

FIG. 1. Transport ρ_{xy} vs total field B_t. (a) $\theta \approx 2.6°$, $T \approx 47$ mK. (b) $\theta \approx 34°$, $T \approx 40$ mK.

above 33°, the high-$B_\perp$ subminimum becomes the main $\nu = \frac{2}{3}$ minimum as the low-$B_\perp$ subminimum ceases to be well defined and disappears. The angle where the two subminima at $\nu \sim \frac{3}{5}$ have equal ρ_{xx}, is within about 2° of 33°, where the $\frac{2}{3}$ subminima have equal ρ_{xx}. The evolution of the $\frac{3}{5}$ subminima as θ increases is less clear than that of the $\frac{2}{3}$ subminima, but will be shown to be generally similar. Though Fig. 2 shows data for a fixed $T \sim 25$ mK, the pairs of subminima for $\nu \sim \frac{2}{3}, \frac{3}{5}$ remain resolved up to $T \sim 100$–200 mK.

Figure 3 summarizes the data on the $B_\perp$ positions of minima in $\rho_{xx}(B_\perp)$ as θ is varied, for two nearly identical states (different cooldowns) of the sample, each with $n \approx 2.4 \times 10^{10}$ cm^{-2}. Each plotted point corresponds to a local minimum in $\rho_{xx}(B_\perp)$; shoulders or inflection points are not shown. The horizontal axis in Fig. 3 is $\nu^{-1} \propto B_\perp$, and the vertical axis is $(\cos\theta)^{-1} = B_t / B_\perp$.

Figure 3 includes data on many angles, so that the angular evolution of a ρ_{xx} subminimum is represented as a continuous, traceable "branch" of points. Branches of subminima just upfield and downfield of $\nu = \frac{2}{3}$ at $\theta \sim 33°$ flow, respectively, toward that exact filling at high and low θ. The high-$B_\perp$ branch persists down to $\theta \approx 23°$, at which angle that subminimum is located nearly 6% upfield of $\nu = \frac{2}{3}$, in the low-$B_\perp$ wing of the stronger $\nu \sim \frac{3}{5}$ minimum. The low-$B_\perp$ branch is well defined only up to 35° or so, but appears to be continued by a shoulder (not shown in Fig. 3) in the low-$B_\perp$ side of the main $\nu \sim \frac{2}{3}$

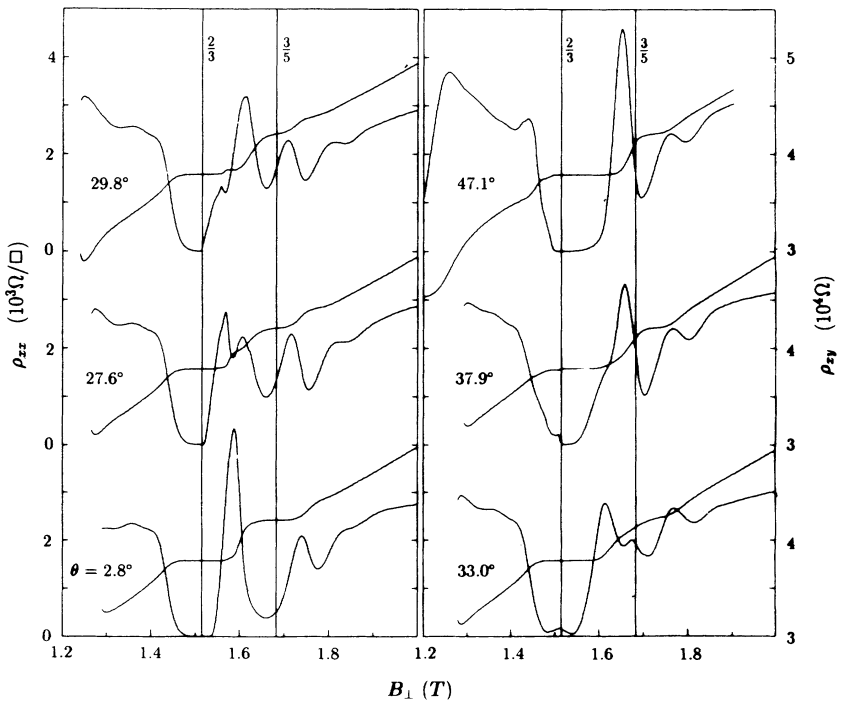

FIG. 2. Transport ρ_{xx}. ρ_{xy} vs perpendicular field with $T \approx 25$ mK, at several angles, showing evolution of the splitting of the ρ_{xx} minima with angle.

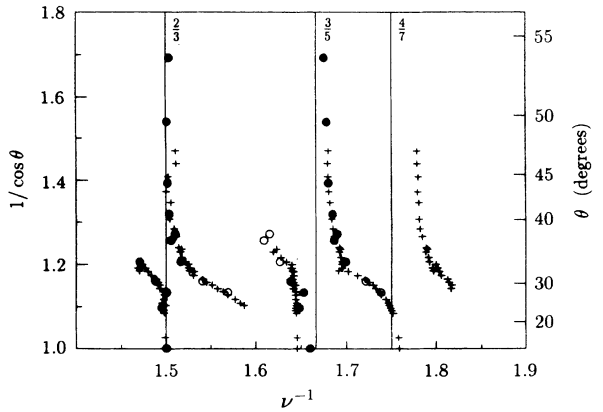

FIG. 3. $1/\cos\theta$ vs ν^{-1} of ρ_{xx} minima for two sample states, both with $n\approx 2.4\times 10^{10}$ cm^{-2}. +, state 1, $T\approx 25$ mK. ○, ●, state 2, $T\approx 50$ mK, where filled-in points correspond to points shown on the $\Delta(B_t)$ curves in Figs. 7 and 8(b).

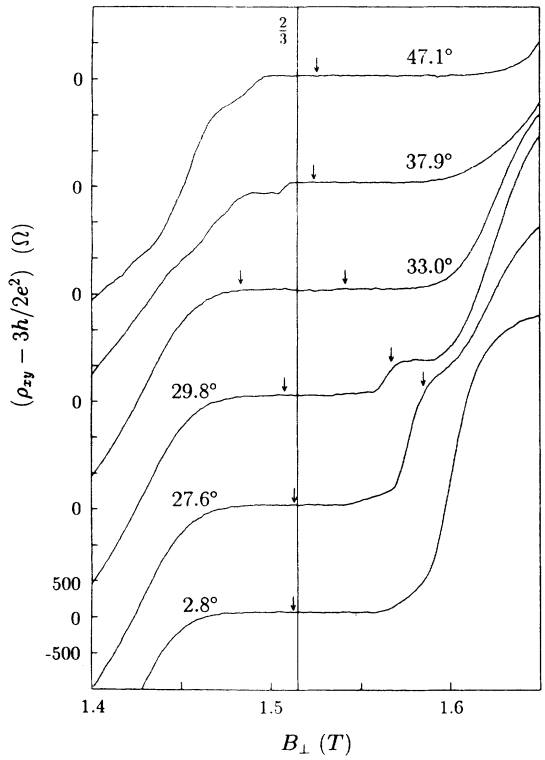

FIG. 4. Transport ρ_{xy} vs perpendicular field for $T\approx 25$ mK, at several angles, showing evolution of the $\frac{2}{3}$ FQHE plateau with angle. Successive curves are displaced by 1500Ω. $\rho_{xy}(B_\perp)$ curves are the same as in Fig. 2, but are enlarged. Arrows indicate the positions of well-developed minima in corresponding $\rho_{xx}(B_\perp)$.

minimum. This shoulder can be seen clearly up to $\theta\approx 43°$, for example, in the 37.9° curve in Fig. 2. Branches of subminima on either side of $\nu=\frac{3}{5}$ for intermediate θ flow likewise toward $\nu=\frac{3}{5}$ for high and low θ, though the field positions converge more slowly than they do for the branches that flow toward $\nu=\frac{2}{3}$. The low-$B_\perp$ branch flows toward $\nu=\frac{3}{5}$ as θ decreases, and is 0.5% downfield of that filling at $\theta\approx 0°$. The high-$B_\perp$ $\nu\sim\frac{3}{5}$ subminimum branch flows toward $\nu=\frac{3}{5}$ at high θ, being about 0.5% upfield of $\nu=\frac{3}{5}$ at $\theta\approx 55°$, but flows into $\nu\approx\frac{4}{7}$ as θ goes to zero. For $\theta>27°$ a different branch of minima appears with ν between $\frac{4}{7}$ and $\frac{5}{9}$.

Even when shifted far from $\nu=\frac{2}{3},\frac{3}{5},\frac{4}{7}$, a well-developed minimum in $\rho_{xx}(B_\perp)$ is generally accompanied by an inflection in $\rho_{xy}(B_\perp)$. An enlarged version of the $\rho_{xy}(B_\perp)$ curves in Fig. 2 is shown in Fig. 4, where the locations of the ρ_{xx} minima are also marked. At all angles surveyed and $T\sim 25$ mK, there is a ρ_{xy} plateau near $\nu=\frac{2}{3}$ that is accurately quantized to $3h/2e^2$ to within our experimental accuracy of 0.2% measured relative to the $\nu=\frac{1}{3}$ plateau, or to within 0.1% relative to the $\nu=\frac{2}{3}$ plateau at $\theta\approx 0°$. At angles where there are two $\rho_{xx}(B_\perp)$ subminima at $\nu\sim\frac{2}{3}$ the accurately quantized plateau accompanies the stronger subminimum, which is always the one whose $B_\perp$ is closer to $\nu=\frac{2}{3}$. For $\theta\approx 33°$, $\rho_{xy}(B_\perp)$ is flat in the region of the $\rho_{xx}(B_\perp)$ subminima, and is accurately quantized. At angles just above or below 33° the weaker subminimum (or shoulder, for $\theta>33°$) is associated with a reasonably flat plateau, such as are seen in the 29.8° and 37.9° curves on Fig. 4. The ρ_{xy} value of this plateau varies continuously with θ and is smaller than $3h/2e^2$ for $\theta>33°$ and larger than $3h/2e^2$ for $\theta<33°$. As θ is increased or decreased further from 33°, the ρ_{xy} plateau associated with the weaker, more shifted ρ_{xx} subminimum (or shoulder) becomes less flat and eventually disappears. It can be seen from Fig. 2 that the $\nu\sim\frac{3}{5}$ plateaus are not as well defined as those for $\nu\sim\frac{2}{3}$, particularly for $\theta\sim 33°$, where $\rho_{xx}(B_\perp)$ shows two subminima. At high and low angles ($\theta<24°, \theta>45°$), though, the $\nu\sim\frac{3}{5}$ plateaus are flat enough to show quantization to within 0.5%.

IV. ENERGY GAPS VERSUS B_t

The splitting of the ρ_{xx} minima at $\nu\sim\frac{2}{3}$ and $\frac{3}{5}$ occurs together with a sharp suppression of the energy gaps that are associated with these minima. We obtained energy gaps by fitting the conductivity σ_{xx} vs T to $\sigma_{xx}(T)=A\exp(-\Delta/2T)$. σ_{xx} was computed from the measured resistivities as $\sigma_{xx}=\rho_{xx}/(\rho_{xx}^2+\rho_{xy}^2)$.

Caution is required in using the formula, $A\exp(-\Delta/2T)$, which produces a linear Arrhenius plot ($\ln\sigma_{xx}$ vs T^{-1}), to fit experimental data. First, Arrhenius plots of data always develop a downward curvature at high T, as a consequence of a high density of excitations, so we always cut off our fits at high T before this downward curvature sets in. Second, the data can show an upward curvature at lower T, so that the full plot is S shaped, rather than linear. The upward curvature at low T is attributed to hopping conduction via localized states near the Fermi level. Various methods exist in the literature for extracting Δ values from such S-shaped Arrhenius plots. Eisenstein *et al.*[11] and Clark *et al.*[9,12] fit only the linear midsection of the Arrhenius plot, where the slope is steepest. Boebinger *et al.*[21] fit $\sigma_{xx}(T)$ data to

four-parameter formulas consisting of an activated term. $A\exp(-\Delta/2T)$, and another two-parameter term to fit the low-T behavior. They used three forms of this low-T term: Ono[22] and Mott[23] hopping conductivity formulas, and another exponentially activated term. In general, if the linear midsection of an Arrhenius plot is long enough, good four-parameter fits can be obtained with any of these low-T terms and the resulting Δ values agree with each other as well as with the Δ from the slope of the linear midsection. This situation, in which all fitting methods give about the same Δ, is typical of the $\sigma_{xx}(T)$ data that we will present.

Figure 5 shows typical Arrhenius plots of $\sigma_{xx}(T)$ data at $\nu\sim\frac{2}{3}$ for several tilt angles. The fit lines shown are from the simple activated formula, and the resulting Δ's are smallest for $B_t\sim1.8$ T, $\theta\sim33°$. The plots in Fig. 5 are linear over factors of 10–100 in σ_{xx}. The linear ranges are shortest at $\theta\approx34.1°$, where Δ's are smallest, and at $\theta\approx62.4°$, the highest angle. The σ_{xx} values shown in Fig. 5 were evaluated at local minima[24] in σ_{xx} vs $B_\perp$. The $\frac{2}{3}$ FQHE σ_{xx} (or ρ_{xx}) minimum is clearly split at $\theta\approx34.1°$, and the σ_{xx} values shown for this angle were evaluated at the subminima lying on either side of $\nu=\frac{2}{3}$.

In Fig. 6 the circles show the splitting of the $\frac{2}{3}$ FQHE at $\theta\approx34.1°$ in a plot of Δ vs ν^{-1}. The two peaks in the data can be identified with the two subminima observed in ρ_{xx} vs $B_\perp$. For comparison, Fig. 6 also shows Δ vs ν^{-1} for $\theta\approx49.5°$, where there is no evidence for splitting in either Δ vs ν or transport data. The single broad peak in the 49.5° Δ vs ν data is centered at $\nu=\frac{2}{3}$, has a width roughly the same as the ρ_{xx} minimum, and can be interpreted[25] by analogy with the integer quantum Hall effect as a consequence of impurity-broadened quasiparticle and quasihole bands. The two peaks in the 34.1° plot of Fig. 6 appear to be formed by a sharp region of decreased Δ splitting a broader background that decreases as ν gets further from $\frac{2}{3}$, and that has about the same width as the $\theta=49.5°$ plot. The central minimum in the 34.1° plot is located at $\nu^{-1}\approx1.49$, where $B_t\approx1.83$ T.

Figure 7 shows a plot of Δ vs B_t for the $\frac{2}{3}$ FQHE, put together with three different kinds of data. The points

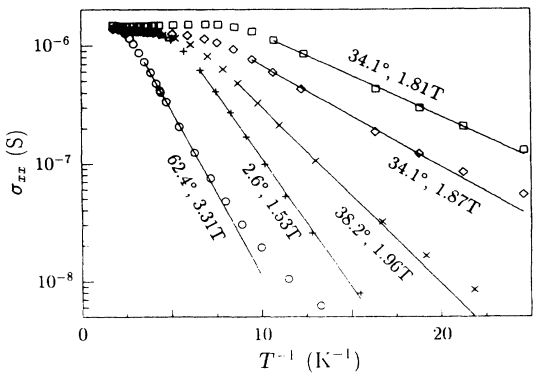

FIG. 5. T dependence of conductivity σ_{xx} for the $\frac{2}{3}$ FQHE, evaluated on well-developed σ_{xx} minima. Arrhenius plots for several angles θ.

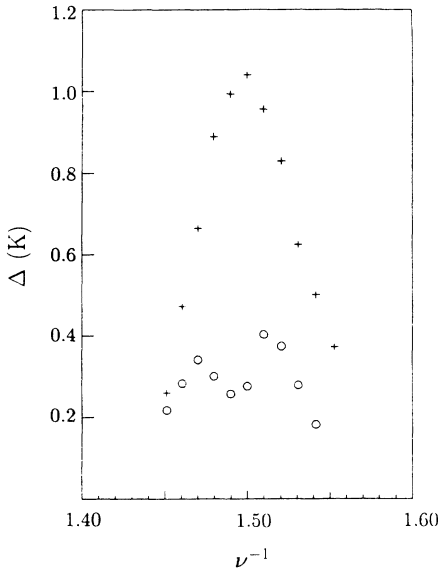

FIG. 6. Dependence of effective gap energy on inverse filling, near $\nu=\frac{2}{3}$. Tilt angle $\theta=49.5°$, +; $\theta=34.1°$, ○.

(+) are from σ_{xx} minima that are not measurably shifted from $\nu=\frac{2}{3}$, and include the data for all angles except 34.1° and 38.2°. The other points on Fig. 7 are from these two angles, with points (○) from σ_{xx} evaluated on minima, and points (×) evaluated at $\nu=\frac{2}{3}$ exactly. The ν^{-1}'s of all the σ_{xx} minima for which Δ's are shown in Fig. 7 are graphed in Fig. 3, as filled circles. All the Δ's shown in Fig. 7 are determined by the simple activated fit, and agree to within about 100 mK with those obtained from all the other fitting methods mentioned above.

The most prominent feature of the plot in Fig. 7 is the minimum at the "critical" B_t of $B_{tc}^{2/3}=1.83\pm0.02$ T, which gives a critical angle $\theta_c\equiv\cos^{-1}(3ne/2hcB_{tc})=33.3\pm1.0°$. This is the same angle where the high- and low-field-split ρ_{xx} subminima are of the same strength.

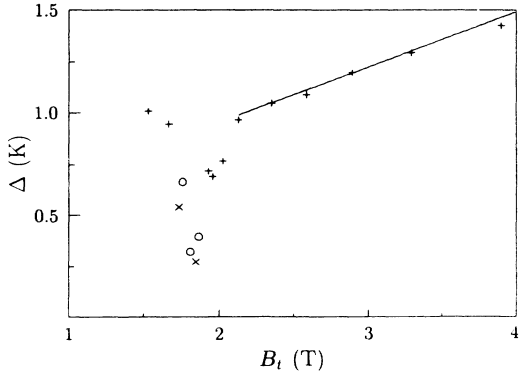

FIG. 7. $\frac{2}{3}$ FQHE gap energy Δ vs total field, +, from essentially unshifted σ_{xx} minima, ○, from shifted minima, ×, from $\nu=\frac{2}{3}$ exactly. The line drawn in for $B_t>2.1$ T has slope 0.27 $K/T=0.4\mu_B\approx g\mu_B$ for GaAs.

For B_t well above the minimum, $B_t > 2.1$ T, the Δ data of Fig. 7 are fit well by a straight line of slope $0.4\mu_B \approx g\mu_B$ for GaAs. The available range of B_t below the minimum is limited, but the data at the lowest B_t's show the sharp increase of Δ with decreasing B_t beginning to saturate.

Typical Arrhenius plots for the σ_{xx} minima at $\nu \sim \frac{3}{5}$ are shown in Fig. 8(a), and Δ vs B_t for $\nu \sim \frac{3}{5}$ is shown in Fig. 8(b). The minimum in Δ vs B_t is located at $B_{tc}^{3/5} = 2.00 \pm 0.05$ T, which gives a critical angle $\theta_c^{3/5} = 31.7° \pm 2.3°$. The maximum linear range for the Arrhenius plots is about a factor of 5 in σ_{xx}. This falls to a factor of 2 near the minimum in Δ vs B_t, while plots for $\theta \geq 38°$ ($B_t \geq 2.2$ T) are essentially curved over the entire T range. The $\Delta(B_t)$ values with $B_t \geq 2.2$ T were determined from four-parameter fits using simple activation together with an Ono hopping term, and agree with $\Delta(B_t)$ from four-parameter fits with the other low-T terms to within 10%. The plot of $\Delta(B_t)$ from the steepest slope of the Arrhenius plots differs from that shown in the figure in that it levels off on the high-B_t side of the minimum at about 150 mK rather than increasing steeply as the curve of Δ from four-parameter fits does.

For the $\frac{3}{5}$ FQHE $\sigma_{xx}(T)$ was evaluated only at minima in σ_{xx} vs $B_\perp$ to obtain the Arrhenius plots and Δ's. These σ_{xx} minima were typically shifted away from $\nu = \frac{3}{5}$ exactly, and Δ's shown in Fig. 8(b) correspond to subminima whose ν^{-1}'s appear in Fig. 3 as filled circles. Subminima in the branch just upfield of $\nu = \frac{3}{5}$ in Fig. 3 have $B_t > B_{tc}^{3/5}$, while subminima in the branch just downfield of $\nu = \frac{3}{5}$ have $B_t < B_{tc}^{3/5}$. Evaluating Δ at $\nu = \frac{3}{5}$ exactly when the σ_{xx} subminima are shifted, as we did for $\nu = \frac{2}{3}$, was not possible because the T dependence of σ_{xx} away from the minima did not allow a reasonable evaluation of Δ.

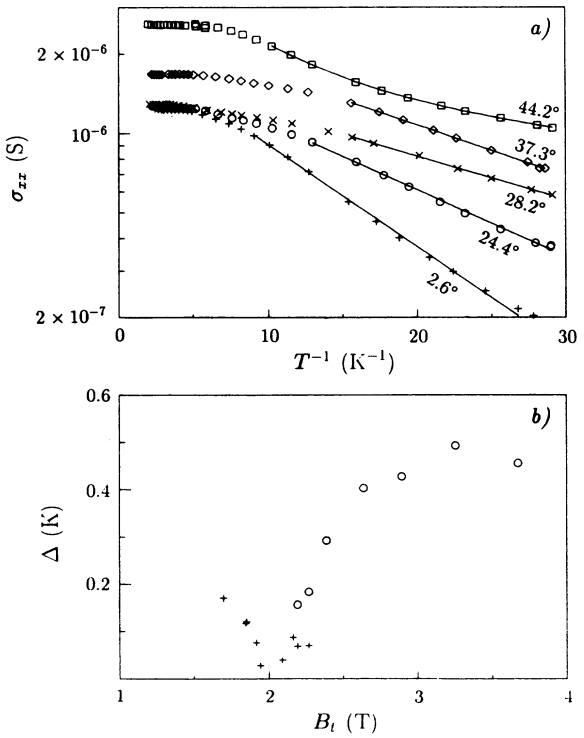

FIG. 8. T dependence of conductivity σ_{xx} for the $\frac{3}{5}$ FQHE. (a) Arrhenius plots for several tilt angles. For clarity the 37° data are multiplied by 1.3, and the 44° data are multiplied by 2. (b) Gap energy Δ vs total field. +, from fit to simple activation; ○, from Ono hopping plus simple activation.

V. RESULTS FOR A HIGHER DENSITY

We also obtained a limited amount of data on a state of the same sample with $n \approx 3.9 \times 10^{10}$ cm^{-2}. At this n the ρ_{xx} minima for the $\frac{2}{3}$ and $\frac{3}{5}$ FQHE develop a splitting only for $\theta < 17°$. For both fractions, the measured Δ increases with B_t, more strongly at lower B_t and θ. The Δ vs B_t data and the splitting of the ρ_{xx} minima for both $\nu \sim \frac{2}{3}$ and $\frac{3}{5}$ resemble those that we observe for $n \approx 2.4 \times 10^{10}$ cm^{-2} at $\theta \gtrsim 33°$. We conclude then, that for this higher density state $B_{tc}^{2/3}$ and $B_{tc}^{3/5}$ are either just above their respective $B_\perp$'s, or are barely too low to be accessible. For the purposes of later discussion we can reasonably take $B_{tc} \sim B_\perp$ for the $\frac{2}{3}$ and $\frac{3}{5}$ FQHE and $n \approx 3.9 \times 10^{10}$ cm^{-2}.

VI. DISCUSSION

We interpret the splitting of the ρ_{xx} minima for the $\frac{2}{3}$ and $\frac{3}{5}$ FQHE and the accompanying minima in Δ vs B_t as effects of a transition of the ground state from a lower to a higher spin as B_t is increased. A sharp minimum in Δ vs B_t occurring at a phase transition suggests that coexistence of the two phases would be energetically favorable in the transition region, and such coexistence must be the cause of the ρ_{xx} subminima that are shifted away from $\nu = \frac{2}{3}$ at $\theta \sim \theta_c$, but which evolve continuously into a well-developed $\nu = \frac{2}{3}$ FQHE at high or low θ. The ground-state spin-transition picture is therefore in accord with our observation of simultaneous weakening and splitting of the FQHE, as well as the theoretical predictions[16–19] that the lowest E_c ground states for $\nu = \frac{2}{3}$ and $\frac{3}{5}$ are not completely polarized.

Phenomenologically, the shifted ρ_{xx} subminima resemble a weak, unshifted FQHE, since they are accompanied by a ρ_{xy} inflection when they are well developed. The difference is that the $B_\perp$'s of the shifted subminima depend on θ, as do the values of ρ_{xy} at the plateaus that can accompany them. In experiments without a detailed survey of ρ_{xx} and ρ_{xy} over many angles a weak, shifted $\frac{2}{3}$ FQHE subminimum could easily be taken for a $\frac{9}{13}$, $\frac{8}{13}$, or $\frac{7}{11}$ FQHE, and it is possible that such shifted subminima may have been observed in earlier studies.[20,26]

We can model the shift of the $\frac{2}{3}$ FQHE ρ_{xx} subminima in more detail by taking the ground-state spin transition to take place at the total field $B_{tc}^{2/3}$ where it is energetically favorable, even when $B_{tc}^{2/3}$ does not fall on $\nu = \frac{2}{3}$ exactly. This is reasonable, since for ν near but not equal to $\frac{2}{3}$ the correlations of the incompressible $\nu = \frac{2}{3}$ ground state are preserved, so that quasiparticles or quasiholes exist

along with the underlying $\nu=\frac{2}{3}$ ground state. As a consequence of phase separation,[27] the spin transition in the underlying state produces a peak in the per electron energy versus ν, $E(\nu)$, on top of the variation of $E(\nu)$ due to the changing density of quasiparticles or quasiholes. A local minimum formed on one side of such a peak in $E(\nu)$ would give rise to a shifted ρ_{xx} minimum and an unquantized ρ_{xy} inflection such as we observe. It is worth noting that the relatively well-developed subminimum that is just upfield of $\nu=\frac{2}{3}$, and that evolves into the main $\nu=\frac{2}{3}$ FQHE at large θ, appears at nearly constant B_t as θ varies from 24° to 30°, and the ν at which the subminimum is located varies by $\sim 4\%$.

Small-system studies by Chakraborty and coworkers[17,19] predict that for both $\nu=\frac{2}{3}$ and $\frac{3}{5}$ a ground-state spin transition is accompanied by a wide region of B_t in which the FQHE energy gap vanishes. The calculations are for $\theta=0$, varying B_t by varying density, and do not allow for any phase separation. For $\nu=\frac{2}{3}$ the predicted width of the gapless region is $0.5B_{tc}$, and for $\nu=\frac{3}{5}$ the width is $0.4B_{tc}$. These predicted relative widths might possibly correspond to full widths of our observed minima in Δ vs B_t, but we observe no region where the gap completely vanishes, and the B_t region where the $\frac{2}{3}$ Δ is less than half its value at the shoulder is only 0.1 T, or 6% of $B_{tc}^{2/3}$ wide, much smaller than the theory predicts.

Well above the transition region, Δ vs B_t for $\nu=\frac{2}{3}$ is a straight line whose slope is approximately $g\mu_B$, which indicates that Zeeman energy corresponding to one electron spin flip is gained on excitation in this range of B_t. The linearly increasing Δ vs B_t is in qualitative agreement with the theory of Chakraborty,[17] which predicts a spin change on excitation from a polarized $\nu=\frac{2}{3}$ ground state. A linear region of $\Delta(B_t)$ for $\nu=\frac{2}{3}$ was not observed by Eisenstein *et al.*[11] whose sample n was ~ 1.5 times ours.

To compare our measured B_t,θ_c with theory and with other experimental results, we will use our B_t,θ_c to calculate δC, the interaction energy difference between the lower- and higher-spin states, expressed in units of $e^2/\epsilon l_\perp$, where $l_\perp$ is the magnetic length $(\hbar c/eB_\perp)^{1/2}$ and ϵ is the dielectric constant of GaAs. Following Eisenstein *et al.*[11] we take the spin transition driven by increasing B_t to entail an E_C increase that compensates exactly for the E_Z decrease caused by the larger polarization, so that at the transition, $\delta C e^2/\epsilon l_{\perp c}=g\mu_B B_{tc}\delta S$, where δS is the spin change per electron on going through the transition.

Given δS from theory, δC can be calculated from an experimental B_{tc},θ_c. For $\nu=\frac{2}{3}$ small-system theoretical studies[16,17] suggest a δS of $\frac{1}{2}$, corresponding to a transition from a completely unpolarized state to a completely polarized one. Using this δS, we calculate $\delta C=0.0039$ and 0.0041, respectively, for $\nu\sim\frac{2}{3}$ transitions in our states with $n\sim 2.4\times 10^{10}$ and 3.9×10^{10} cm^{-2}. We assumed $B_\perp(\nu=\frac{2}{3})\sim B_{tc}^{2/3}$ for the state with $n\approx 3.9\times 10^{10}$ cm^{-2}. Other experimental δC values calculated for $\nu=\frac{2}{3}$ transitions[11,12] agree closely with each other, and are about 0.0048, and estimates of δC for $\nu=\frac{2}{3}$ from small-systems calculations[16,17] are about 0.010. For $\nu=\frac{3}{5}$ a six-electron calculation[19] predicts that the spin transition on increasing B_t is from a total spin of one to a total spin of three. Using $\delta S=\frac{1}{3}$, we obtain $\delta C\approx 0.0027$ for $n\approx 2.4\times 10^{10}$ cm^{-2}, and $\delta C\approx 0.0030$ for $n\approx 3.9\times 10^{10}$ cm^{-2}, compared with a theoretical estimate[19] of $\delta C\approx 0.0086$. For both fractions, the larger theoretical δC values can be attributed to the calculations having neglected the finite thickness of the 2DES, whose effect is to reduce energies of FQHE states. Sample-dependent 2DES thickness and disorder can explain the small discrepancies between the experimental δC values, so the available experimental and theoretical estimates of δC are consistent with the interpretation of the minima observed in $\Delta(B_t)$ as ground-state spin transitions.

VII. CONCLUSIONS

To summarize, we have observed a θ-dependent splitting in the $\frac{2}{3}$ and $\frac{3}{5}$ FQHE. The splitting is associated with minima in Δ vs B_t, and can produce ρ_{xx} minima and ρ_{xy} inflections that are shifted well away from $\nu=\frac{2}{3}$ or $\frac{3}{5}$. This behavior could be produced by phase separation occurring in a narrow B_t region where there is a ground-state spin transition. In plots of Δ vs B_t minimum for the $\frac{2}{3}$ FQHE is sharp and deep, and the minimum for the $\frac{3}{5}$ effect is the first to be observed. The critical fields and angles B_{tc},θ_c at which these minima in Δ vs B_t are observed are consistent with the minima being produced by a ground-state spin transition. With $2.1<B_t<4$ T, the $\nu=\frac{2}{3}$ Δ vs B_t plot is linear, with a slope that indicates Zeeman energy corresponding to one electron spin flip is gained on excitation.

Note added in proof. Since submitting this paper, it has come to our attention that a paper by R. G. Clark in *Localization and Confinement of Electrons in Semiconductors,* edited by F. Kuchar *et al.* (Springer, Berlin, 1990) shows Δ vs B_t for the $\frac{2}{3}$ FQHE, and a plot of angular evolution of the positions of ρ_{xx} minima for the $\nu\sim\frac{2}{3}$ region.

ACKNOWLEDGMENTS

We thank M. Santos for assistance in sample growth. This work was supported by NSF Grants Nos. DMR-90162 and DMR-8921073, and a grant from the NEC corporation.

[1]D. C. Tsui, H. L. Stormer, and A. C. Gossard, Phys. Rev. Lett. **48**, 1559 (1982).
[2]R. B. Laughlin, Phys. Rev. Lett. **50**, 1395 (1983).
[3]B. I. Halperin, Helv. Phys. Acta **56**, 75 (1983).
[4]T. Chakraborty and F. C. Zhang, Phys. Rev. B **29**, 7032 (1984).
[5]F. C. Zhang and Tapash Chakraborty, Phys. Rev. B **30**, 7320 (1984).
[6]R. J. Haug, K. v. Klitzing, R. J. Nicholas, J. C. Maan, and G. Weimann, Phys. Rev. B **36**, 4528 (1987).
[7]J. P. Eisenstein, R. L. Willett, H. L. Stormer, D. C. Tsui, A. C.

Gossard, and J. H. English, Phys. Rev. Lett. **61**, 997 (1988).
[8]J. E. Furneaux, D. A. Syphers, and A. G. Swanson, Phys. Rev. Lett. **63**, 1098 (1989).
[9]R. G. Clark, S. R. Haynes, A. M. Suckling, J. R. Mallet, P. A. Wright, J. J. Harris, and C. T. Foxon, Phys. Rev. Lett. **62**, 1536 (1989).
[10]J. P. Eisenstein, H. L. Stormer, L. N. Pfeiffer, and K. W. West, Phys. Rev. Lett. **62**, 1540 (1989).
[11]J. P. Eisenstein, H. L. Stormer, L. N. Pfeiffer, and K. W. West, Phys. Rev. B **41**, 7910 (1990).
[12]R. G. Clark, S. R. Haynes, J. V. Branch, A. M. Suckling, P. A. Wright, P. M. W. Oswald, J. J. Harris, and C. T. Foxon, Surf. Sci. **229**, 25 (1990).
[13]T. Chakraborty and P. Pietiläinen, Phys. Rev. B **39**, 7971 (1989).
[14]V. Halonen, P. Pietiläinen, and T. Chakraborty, Phys. Rev. B **41**, 10 202 (1990).
[15]T. Chakraborty, P. Pietiläinen, and F. C. Zhang, Phys. Rev. Lett. **57**, 130 (1986).
[16]X. C. Xie, Yin Guo, and F. C. Zhang, Phys. Rev. B **40**, 3487 (1989).
[17]T. Chakraborty, Surf. Sci. **229**, 16 (1990).
[18]P. A. Maksym, J. Phys. Condens. Matter **1**, 6299 (1989).
[19]T. Chakraborty and P. Pietiläinen, Phys. Rev. B **41**, 10 862 (1990).
[20]T. Sajoto, Y. W. Suen, L. W. Engel, M. B. Santos, and M. Shayegan, Phys. Rev. B **41**, 8449 (1990).
[21]G. S. Boebinger, H. L. Stormer, D. C. Tsui, A. M. Chang, J. C. M. Hwang, A. Y. Cho, C. W. Tu, and G. Weimann, Phys. Rev. B **36**, 7979 (1987).
[22]Y. Ono, J. Phys. Soc. Jpn. **51**, 237 (1982).
[23]N. F. Mott and E. A. Davis, *Electronic Properties in Non-Crystalline Materials* (Clarendon, Oxford, 1989), 2nd ed.
[24]For both the $\frac{2}{3}$ and $\frac{3}{5}$ FQHE, the $B_{\perp}$'s of those subminima, that are well developed enough to allow reasonable evaluation of a Δ, do not shift with T in the T range relevant to measuring Δ.
[25]A. M. Chang, M. A. Paalanen, D. C. Tsui, H. L. Stormer, and J. C. M. Hwang, Phys. Rev. B **28**, 7979 (1983).
[26]V. J. Goldman and M. Shayegan, Surf. Sci. **229**, 10 (1990).
[27]D. Yoshioka (private communication). Yoshioka has considered gapless excitations associated with boundaries between the polarized and unpolarized phases when they coexist.